

A method for unique phase retrieval of ultrafast optical fields

To cite this article: Birger Seifert and Heinrich Stolz 2009 *Meas. Sci. Technol.* **20** 015303

View the [article online](#) for updates and enhancements.

Related content

- [Unambiguous ultrashort pulse reconstruction from double spectrograms alone](#)
Birger Seifert, Robert Alastair Wheatley, Ricardo Rojas-Aedo et al.
- [PhD Tutorial](#)
Antoine Monmayrant, Sébastien Weber and Béatrice Chatel
- [Sub-5 fs optical pulse characterization](#)
Ryuji Morita, Masakatsu Hirasawa, Naoki Karasawa et al.

Recent citations

- [Single-shot laser pulse reconstruction based on self-phase modulated spectra measurements](#)
Elena A. Anashkina *et al*
- [Unambiguous ultrashort pulse reconstruction from double spectrograms alone](#)
Birger Seifert *et al*
- [Reliable multiple-pulse reconstruction from second-harmonic-generation frequency-resolved optical gating spectrograms](#)
A. Hause *et al*

A method for unique phase retrieval of ultrafast optical fields

Birger Seifert^{1,2} and Heinrich Stolz¹

¹ Institut für Physik, Universität Rostock, D-18051 Rostock, Germany

² Facultad de Física, Pontificia Universidad Católica de Chile, Casilla 306, Santiago 22, Chile

E-mail: bseifert@fis.puc.cl

Received 28 April 2008, in final form 7 November 2008

Published 11 December 2008

Online at stacks.iop.org/MST/20/015303

Abstract

A self-referencing technique for measuring amplitude and phase of ultrashort laser pulses is presented. In contrast to the other methods the relative-phase ambiguities do not appear in our method. Thus, we can characterize ultrashort pulses with well-separated frequency components. The relative-phase ambiguities can be avoided by the use of a cross-correlation technique with two independent laser pulses. Further we propose and demonstrate experimentally a new realtime phase-retrieval algorithm that reconstructs both pulses fast and uniquely.

Keywords: ultrafast optical fields, phase retrieval, numerical optimization

(Some figures in this article are in colour only in the electronic version)

1. Introduction

Interferometric and noninterferometric methods have been developed for the full characterization of ultrashort optical signals as complex electric fields. While the spectral phase interferometry for direct electric field reconstruction (SPIDER [1]) or measurement of electric field by interferometric spectral trace observation (MEFISTO [2, 3]) as interferometric methods allow field reconstruction by algebraic inversion algorithms, noninterferometric spectrographic techniques such as frequency-resolved optical gating (FROG [4, 5]) or temporal analysis of spectral components (TASC [6, 7]) rely on the solution of a phase-retrieval problem.

Ultrashort pulses with well-separated frequency components as shown in figure 1 cannot be recovered by any of these self-referenced methods (including SPIDER and MEFISTO) due to relative-phase ambiguities as discussed in [8]. The phase reconstruction procedure of SPIDER involves a step referred to as ‘concatenation’ [1, 9], basically a numerical integration of the derivative of the spectral phase. However, the spectral phase is undefined between well-separated components in the frequency domain. Therefore, SPIDER is prone to suffer from undetermined spectral phase jumps, and hence ambiguous temporal profiles. In order to illustrate this, we show in figure 1 an explicit example in the frequency domain and in the time domain. The π jump in the spectral

phase changes the modulus of the double pulse in the time domain. Instead of the π jump any other phase jump could also appear and yield different double pulses in the time domain. Numerical integration causes the same problems in techniques such as MEFISTO [2] and blind-MEFISTO [3].

The principal task of a pulse characterization technique should be the characterization of arbitrary pulses because there are many experiments where completely unknown ultrashort pulses are generated [10]. Ultrashort pulses with well-separated frequency components appear rather frequently (e.g. in soliton molecules [11] or in the secondary emission from semiconductor quantum wells [12]).

Non-self-referenced methods (e.g. the non-self-referenced variants of FROG and SPIDER such as XFROG [13] and XSPIDER [14, 15]) require well characterized reference pulses and are therefore not applicable in all cases. It can be laborious to characterize reference pulses in a given setup. Moreover measurement errors of the reference pulses propagate into the final result. Nevertheless, there is no general guarantee that XFROG gives a unique field reconstruction [16].

Another cross-correlation technique is blind-FROG [5, 17]. Blind-FROG works with two independent and arbitrary laser pulses without *a priori* knowledge. Unlike XFROG and XSPIDER, blind-FROG is a self-referenced

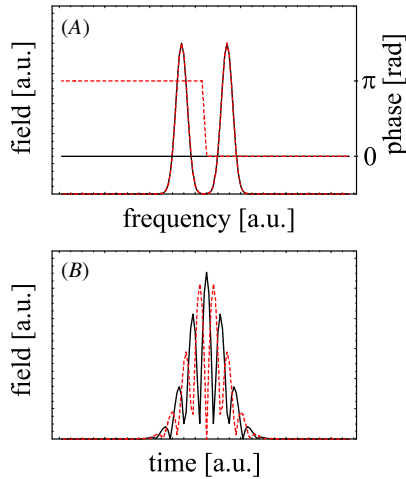


Figure 1. Two double pulses with different spectral phase functions. Here with a π jump at a spectral position with low intensity. (A) Modulus and phase in the frequency domain. (B) Modulus of the two double pulses in the time domain.

method and unlike blind-MEFISTO, blind-FROG requires no spectral overlap between the two independent laser pulses. But blind-FROG faces two serious problems, that of uniqueness, i.e. under which mathematical constraints a unique solution exists, and the problem of the reconstruction algorithm. The latter issue has been under intense discussion (see, e.g., [17]) in the last years. All known algorithms have the drawback of slow convergence and stagnation (see table 1 of [17]). In reality, the former problem is much more severe, as no algorithm can reconstruct lost information. The issue of the uniqueness of several schemes suggested for FROG and TASC has been thoroughly analyzed only recently [16]. The result of this analysis is that from a FROG measurement in general the fields are not uniquely reconstructable. This remains true even when one employs the additional information about the spectral intensities of the pulses, obtained from independent measurements. However, the derived ambiguities do not appear with non-centro-symmetric spectrograms and suitable constraints of the spectral pulse intensity of one of the pulses in the blind-FROG scheme. The relative-phase ambiguities can be avoided in this way. Based on this knowledge, we developed a new technique for the full characterization of arbitrary complex-shaped ultrashort optical signals.

A successful characterization of ultrashort laser pulses with a new technique is presented in this paper. We introduce a new phase reconstruction algorithm which generally converges even for complex and noisy pulses. It is fast and reconstructs ultrashort laser pulses with well-separated frequency components without ambiguities or stagnations. We show a simulation with such pulses and compare the new algorithm with the well-known PCGP algorithm [17]. Furthermore, we have reconstructed the spectral phases of chirped Gaussian pulses in an experimental setup by the application of our method.

Recently, our technique was successfully applied to characterize soliton molecules experimentally [11].

2. The VAMPIRE technique

We have found that the uniqueness issue [8, 16] can be solved efficiently by a cross-correlation technique with two independent and arbitrary laser pulses without *a priori* knowledge. This is because in such a scheme one of the pulses can be modified to prevent any ambiguities while the other pulse remains unchanged. The new self-referencing technique that we present in this paper, and which we suggest to label a very advanced method for phase and intensity retrieval of e-fields (VAMPIRE), is a spectrographic technique. A VAMPIRE spectrogram can be written as a two-dimensional function of time and frequency:

$$I(\Omega, \tau) \propto \left| \int_{-\infty}^{\infty} d\omega G(\omega, \Omega) \exp\{iP(\omega, \Omega)\} \exp(i\omega\tau) \right|^2, \quad (1)$$

where we define

$$G(\omega, \Omega) = |\tilde{E}_1(\omega)| |\tilde{E}_2(\Omega - \omega)|, \quad (2)$$

$$P(\omega, \Omega) = \phi_1(\omega) + \phi_2(\Omega - \omega), \quad (3)$$

with the spectral phases ϕ_1 and ϕ_2 of the pulses.

The conditioning filter is the key element in the typical VAMPIRE arrangement as shown in figure 2. A temporal phase modulator and a spectral phase modulator are two successive parts of the conditioning filter.

2.1. The spectral phase modulator

An unbalanced Mach-Zehnder interferometer (MZI) can be used as a spectral phase modulator. Two replicas of signal 2 in figure 2 are generated. One of the replicas is changed by a dispersive element, for example, a slab of fused silica in one arm of the MZI. The linear response of such a MZI is given by the complex transfer function

$$R_{\text{MZ}}(\omega) \propto (1 + Q \exp[i\tilde{q}(\omega)]). \quad (4)$$

Here $\tilde{q}(\omega)$ is the sum of the spectral phase function of the dispersive element and the linear spectral phase corresponding to the different arm lengths of the MZI. The constant Q determines the splitting ratio. For the characterization of signal 1 in figure 2 it is not necessary to characterize the conditioning filter exactly; $R_{\text{MZ}}(\omega)$ may be unknown and just some qualitative properties of the generated spectrograms should be fulfilled. A sufficient temporal distance between the two replicas from the MZI gives the zero line shown in figure 3 in the VAMPIRE spectrogram. The intensity at the zero line is negligible. In this way, non-centro-symmetric spectrograms (no centro-symmetry for each Ω) can be generated with an unbalanced MZI. The phase function $\tilde{q}(\omega)$ should be at least quadratic, otherwise no additional information would be available. The temporal distance between the two replicas should not be too large so as to avoid sampling problems and to get rid of too many fringes in the spectrum of the filtered signal 2.

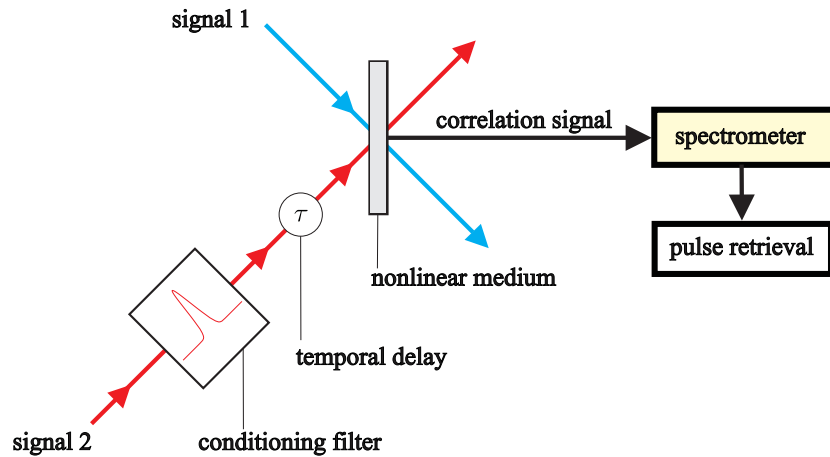


Figure 2. Optical scheme of the VAMPIRE technique.

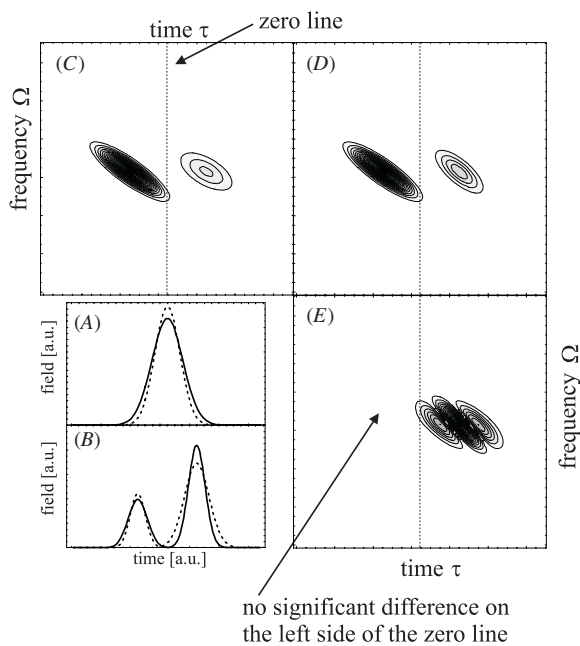


Figure 3. (A) Signal 1 (test pulses). The solid line: $a_1 = -1$, $b_1 = 4$. The dashed line: $a_1 = -1$, $b_1 = 3.2$. (B) Signal 2 (filtered pulses). Without filtering the pulses are defined as follows: the solid line: $a_1 = -4$, $b_1 = -2$. The dashed line: $a_1 = -4$, $b_1 = -5.2$. Without filtering the solid line pulse pair and the dashed line pulse pair yield analytically identical spectrograms. The filtered solid line pulse pair generates the VAMPIRE spectrogram in (C) and the filtered dashed line pulse pair generates the VAMPIRE spectrogram in (D). (E) Modulus of the difference between the VAMPIRE spectrograms in (C) and (D). A grid with 128×128 points has been used.

To give a simple example, for the signals 1 and 2 in figure 2 we choose the electric fields

$$\begin{aligned} \tilde{E}_1(\omega) &= \exp[(\tilde{a}_1 + i\tilde{b}_1)\omega^2] \\ \tilde{E}_2(\omega) &= \exp[(\tilde{a}_2 + i\tilde{b}_2)\omega^2] \end{aligned} \quad (5)$$

with the parameters \tilde{a}_1 , \tilde{b}_1 , \tilde{a}_2 and \tilde{b}_2 defining two different pulse pairs for nontrivial ambiguities as derived in [16]. By construction, the first pulse pair has exactly the same spectral intensities as the second one. The unfiltered signal 1, the filtered signal 2 and the two corresponding

VAMPIRE spectrograms are shown in figure 3. The two VAMPIRE spectrograms are different for the two different pulse pairs; however, two usual XFROG spectrograms are indistinguishable as shown in the left side of the zero line in figure 3(E). The main property of a VAMPIRE spectrogram is the non-centro-symmetry as demanded in [16] for the uniqueness. $|\tilde{E}_2|$ in (2) and ϕ_2 in (3) are changed by the conditioning filter for that purpose but $|\tilde{E}_1|$ and ϕ_1 remain unchanged.

2.2. The temporal phase modulator

The spectral phase modulator avoids ambiguities caused by the symmetry properties of the measured VAMPIRE traces. However, it cannot avoid relative-phase ambiguities. Ultrashort pulses with well-separated frequency components generate relative-phase ambiguities caused by traces with very low intensities between spectral components in the trace as described in [8, 16]. This problem can be solved by a cross-correlation technique such as VAMPIRE because signal 2 in figure 2 can be modified to prevent low intensities between spectral components in the trace. The spectrum of signal 1 has to be covered by the spectrum of signal 2, and there should be no gaps in the spectrum of signal 2. The central frequencies of signals 1 and 2 have not to be equal, and it is not necessary to characterize signal 2 exactly. Such a signal 2 could be generated by an external and independent fs-oscillator.

However, there is a way to generate a suitable signal 2 without an external source. The idea is to use a part of signal 1, generated by a beamsplitter, and to modify its spectrum. This can be done with a temporal phase modulator, such as a self-phase modulation introduced by the Kerr nonlinearity of an optical fiber. That way the spectral bandwidth of ultrashort pulses with well-separated frequency components can be broadened.

3. Reconstruction of the pulses

3.1. Reconstruction algorithm

To reconstruct the pulses the function $G(\omega, \Omega)$ has to be known, i.e. the spectral pulse intensities are added as

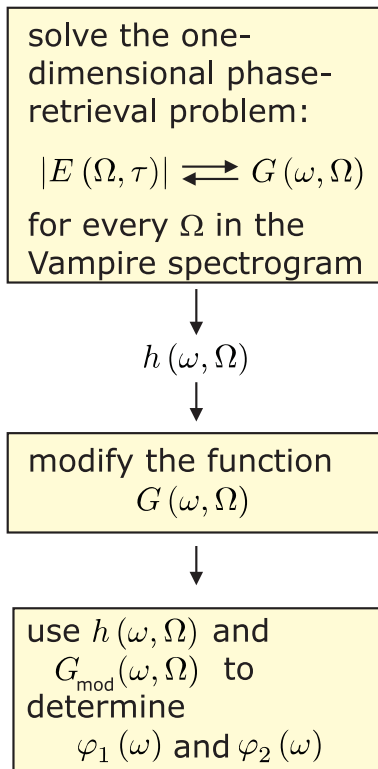


Figure 4. Block diagram of the new phase-retrieval algorithm.

constraints to the problem. So the functions $I(\Omega, \tau)$ and $G(\omega, \Omega)$ are given and the phase functions ϕ_1 and ϕ_2 have to be reconstructed.

Based on the idea for the uniqueness proof in [16] a new phase-retrieval algorithm can be developed. The block diagram of this algorithm is depicted in figure 4. To start the algorithm, we solve the one-dimensional phase-retrieval problem,

$$|E_\Omega(\tau)| = \left| \int_{-\infty}^{\infty} d\omega G_\Omega(\omega) \exp\{iP_\Omega(\omega)\} \exp(i\omega\tau) \right|, \quad (6)$$

for every Ω in the first step. The input of the algorithm is the function $|E(\Omega, \tau)|$, given by the square root of the measured VAMPIRE spectrogram, and the function $G(\omega, \Omega)$, given by the measured spectra of the pulses. When a solution for one of the given one-dimensional phase-retrieval problems is found, it can be used as an initial function for the next one. In this way, we always provide very good initial guesses and can therefore use the Gerchberg–Saxton algorithm [18] with a strongly reduced probability of stagnation for this step. This kind of problem solving yields excellent convergence and significantly improves the performance of the algorithm. In this way one gets the function $h(\omega, \Omega) = P(\omega, \Omega) + F(\Omega)$ with P defined in equation (3) and F being an arbitrary function [16]. By construction the input functions $|E(\Omega, \tau)|$ and $G(\omega, \Omega)$ are non-centro-symmetric and thus P is unique. Noise or distortions in the VAMPIRE spectrogram, or even staginations of the phase-retrieval algorithm for (6), could cause unacceptable errors, so G is modified in the second step of the algorithm by, e.g., omitting this set of data. This can be done because the problem of decomposing $h(\omega, \Omega)$ yields

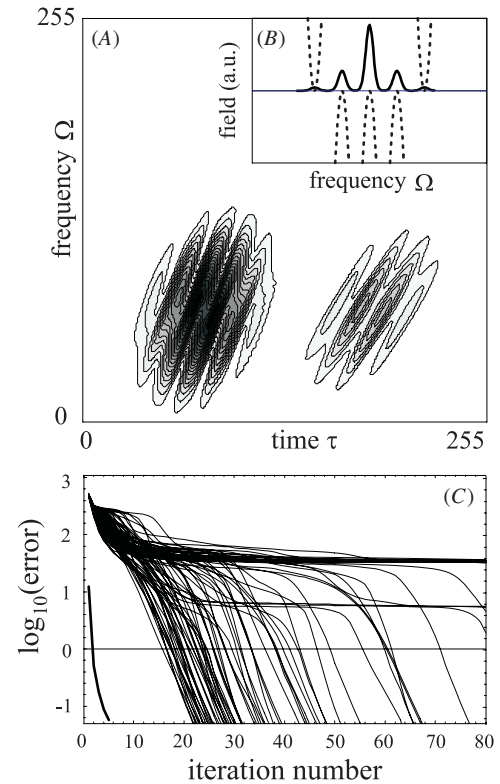


Figure 5. (A) Vampire spectrogram generated with the signal in (B) and a filtered single Gaussian on a grid with 512×512 points. The signal in (B) is a pulse with well-separated frequency components. (C) Rate of convergence plots. 100 plots on the right side show the convergence behavior of the PCGP algorithm [17] for random start values, and one plot in the left lower corner shows the convergence of the new algorithm which is independent of the start values. The quality of the retrieved signals is acceptable below the straight line.

an overdetermined linear system of equations. The modified function G_{mod} and the function h are subsequently sent to the third step of the algorithm where despite the indefiniteness of the function F , h is uniquely decomposed into ϕ_1 and ϕ_2 by a singular value decomposition algorithm.

3.2. Comparison with the PCGP algorithm

To compare the new algorithm with the well-known PCGP algorithm [17] we used a rather complex pulse,

$$E_1(\omega) = \exp[(-0.03 - 0.02i) \times (\omega - N/2)^2] + 0.3 \exp[(-0.03 - 0.02i) \times (\omega - N/2 - 30)^2] + 0.3 \exp[(-0.03 - 0.02i) \times (\omega - N/2 + 30)^2] + 0.05 \exp[(-0.03 + 0.02i) \times (\omega - N/2 - 60)^2] + 0.05 \exp[(-0.03 + 0.02i) \times (\omega - N/2 + 60)^2], \quad (7)$$

consisting of a superposition of five Gaussian spectra which represent well-separated frequency components as shown in figure 5(B). As a second pulse we took a single Gaussian pulse,

$$E_2(\omega) = \exp[-0.0005 + 0.002i) \times (\omega - N/2)^2], \quad (8)$$

which is modified by the conditioning MZI filter (ratio $Q = 0.5$, temporal distance 110 points, referred to a grid of $512 \times$

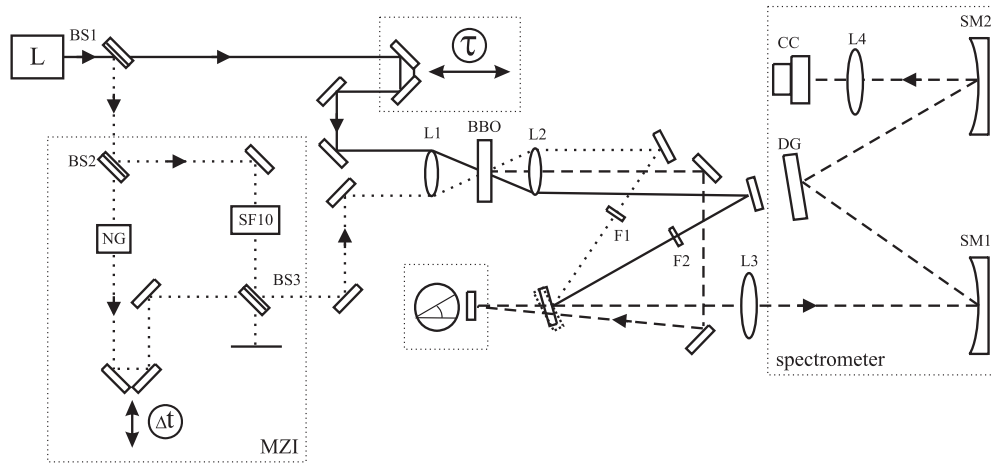


Figure 6. VAMPIRE setup. BS: beamsplitters, NG: neutral density glass filter, SF10: 15 mm thick SF10 glass, MZI: Mach–Zehnder interferometer, L1: lens with a focal length of 50 mm, L2, L3: lenses with a focal length of 75 mm, L4: cylindrical lens with a focal length of 80 mm, BBO: 300 μm thick type I BBO crystal, F: neutral density glass filter, SM: spherical mirror with a radius of curvature of 200 mm, DG: reflecting diffraction grating (150 grooves per mm), CC: 8-bit CMOS camera.

512 points, $N = 512, 0 \leq \omega \leq N - 1$). The nonlinear part of the spectral phase function of the dispersive element in the MZI is given by

$$\tilde{q}_{\text{nonlinear}}(\omega) = 0.0018 \times (\omega - N/2)^2. \quad (9)$$

In figure 5(C), we show the rms FROG error [5] versus the number of iterations, where one iteration is a complete reconstruction cycle consisting of Fourier transforming the data back and forth. Despite the uniqueness, the PCPG algorithm (including the spectra as additional constraints) shows the well-known problems of slow convergence and stagnation. On average more than 40 steps are needed to achieve acceptable errors, and a considerable fraction of iterations does not give convergence. In contrast, the new algorithm is always converging within a few steps.

We have found this fast convergence for simulated VAMPIRE spectrograms generated from a substantial set of different and complex-shaped pulse pairs. Additive and multiplicative noise was added to both the trace and the spectra. The speed of the algorithm is fast even for very large VAMPIRE grids up to 1024×1024 points. The second and third steps are much faster than the first step of the algorithm. Further speed improvements of the first step are expected with new numerical methods [19] for the solution of (6).

3.3. The chirp z -transform

The spectra and traces are usually measured with CCD detectors or CMOS detectors and are therefore arrays of data points. As many points as possible should be used to increase the resolution and to decrease sampling effects. It is well known that the broader the peak of a function (e.g. in the frequency domain), the narrower the Fourier transform (e.g. in the time domain). Therefore, there are often many unused points in the trace arrays. ‘Unused’ means that the points contain the background noise. This problem can be solved by replacing the usual discrete Fourier transform (DFT) with a

chirp z -transform [20, 21] (CZT). The CZT is given by

$$\tilde{f}(k) = \sum_{n=0}^{N-1} f(n) \exp\left(i \frac{2\pi}{N} nk\alpha\right) \quad \text{for } 0 \leq k \leq N - 1 \quad (10)$$

and is identical to the DFT for $\alpha = 1$. The width of the discrete signal $\tilde{f}(k)$ in (10) can be changed by the arbitrary scalar value α . The smaller the α the broader is the signal $\tilde{f}(k)$. With the CZT the signals can be broad in the frequency domain and in the time domain simultaneously. The VAMPIRE trace can be blown up in that way.

For a sensitive measurement of the spectral phase one should ensure a high spectral resolution. In that case many points on the frequency axis will contain useful information. Gaussian pulses with weak chirp will generate very narrow traces on the time axis when the DFT is used. The discretization error due to the sampling on the given grid cannot be neglected anymore and can result in poor reconstructions. The CZT solves this problem. Corresponding measured VAMPIRE traces are shown in the following section. On the one hand, the CZT reduces discretization errors and despite small grids it makes it possible to increase the spectral resolution of the spectral phase. On the other hand, the CZT necessitates more calculations and thus more time for the reconstruction. We replaced the DFT in the Gerchberg–Saxton algorithm by the CZT. This almost quarters the speed, but it is acceptable for us due to the high performance of the new algorithm.

Finally, we note that a larger grid size generally increases the resolution. However, in practice, the size of the grid is limited by the detector and cannot be increased arbitrarily. Thus, one should use as many points as possible of the given grid.

4. Experimental setup and results

Figure 6 shows a schematic of the VAMPIRE arrangement. The beamsplitter BS1 splits the beam from our homemade

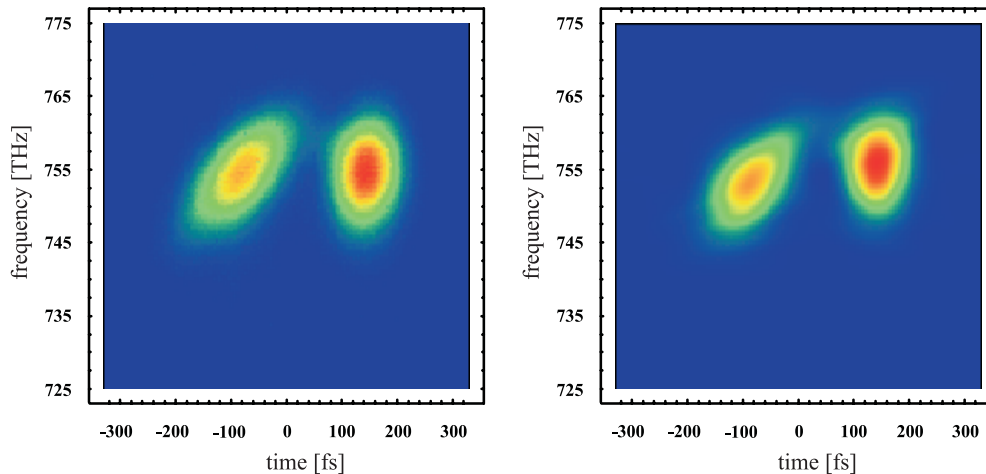


Figure 7. Two 128×128 pixel traces. The left VAMPIRE trace is a measured trace, and the right VAMPIRE trace is the corresponding reconstructed trace.

Ti:sapphire laser oscillator into two parts. One part passes the MZI while the other one is running through a translation stage. The pulses are brought back together and focused into a $300 \mu\text{m}$ thick type I BBO crystal. The generated sum-frequency light and the two fundamental beams are frequency resolved by a Czerny–Turner spectrometer. The sum-frequency light is detected in the second order of the grating, and the spectra of the pulses are detected in the first order. In this way, the spectra of the pulses and the VAMPIRE traces can be measured simultaneously. The spectrometer camera is a triggered 8-bit CMOS camera and transmits the images to a computer where the data are processed and visualized by a Delphi 5 program. Synchronized moving iron loudspeakers were used for the translation stage and for the generation of a tilt angle of the sum-frequency beam. Thus, the frequency-resolved sum-frequency beam moving up and down is generating the VAMPIRE traces on the chip of the camera. Lens L4 in front of the camera is a cylindrical lens for the astigmatism compensation in the Czerny–Turner spectrometer. The setup in figure 6 is a prototype of the VAMPIRE technique. It can be enhanced by replacing the speakers with piezo-driven positioning systems because the linearity of the generated time axis is degraded by the use of speakers. The prototype is a multishot configuration but a single-shot arrangement should be straightforward.

Figure 7 shows measured and reconstructed VAMPIRE traces. The agreement is quite good. The left parts of the traces acquired a tilt from the chirp generated in one arm of the MZI. The speed of 10 reconstructions per second on a 1.4 GHz Intel Pentium computer was not optimal because the reconstruction and the trace measurement were not simultaneously initiated and stopped. Note that the time axis is stretched by a factor 3.85 due to the value $\alpha = 0.26$ in the CZT, by which a considerable improvement in the temporal or spectral resolution is obtained. The reconstructed pulses are not used as improved initial values for the next reconstruction. Every reconstruction is independent of the previous one. The retrieved pulses are shown in figure 8. Signal 1 in figure 2 is usually the signal to be characterized and appears in figure 8(A) as a single Gaussian pulse. The phase obtained

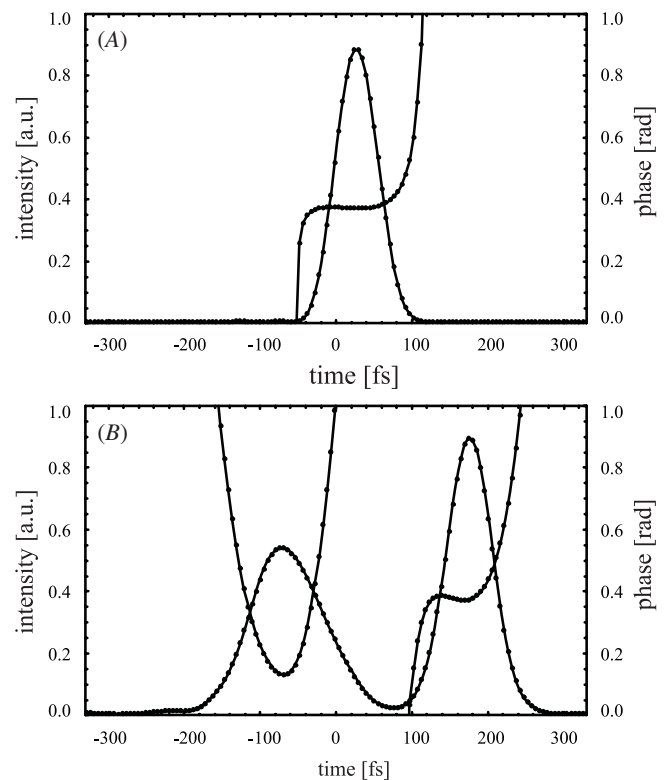


Figure 8. (A) Retrieved signal 1 with a FWHM of 64 fs. (B) Retrieved signal 2 with a FWHM of 113 fs for the left Gaussian and a FWHM of 71 fs for the right Gaussian.

shows that our laser provides pulses that are transform limited. The central wavelength of the pulses is 800 nm. The group-velocity dispersion of SF10 glass at 800 nm is $\beta^{(2)} = 1566 \text{ fs}^2 \text{ cm}^{-1}$ and can be calculated from the Sellmeier dispersion formula [22]. For a $L = 1.5 \text{ cm}$ thick SF10 glass one gets a group-delay dispersion (GDD) of $\beta^{(2)}L = 2349 \text{ fs}^2$. A comparison of the reconstructed pulses from the two arms of the MZI (the two Gaussians of signal 2 in figure 8(B)) gives a stretch factor of $113 \text{ fs}/(71 \text{ fs}) = 1.59$. The theoretical stretch factor calculated from the GDD of the SF10 glass is 1.63. The deviation from the measured value is less than 3%.

One reason for the deviation is that the pulses from the MZI arm without SF10 glass have a weak linear chirp caused by the dispersion of the beamsplitters and of the neutral density glass NG, which defines the constant Q in (4). However, the calculated theoretical stretch factor is based on transform-limited Gaussian pulses. Another reason for the deviation is the weak nonlinear time axis due to the speakers.

5. Discussion and conclusions

We have demonstrated a new self-referencing technique for simultaneously measuring the amplitude and phase of two independent ultrashort laser pulses. It is different from recently developed reconstruction techniques [5, 17, 23] because a conditioning filter is used which guarantees the uniqueness of reconstruction. For the characterization of just one signal it is not even necessary to characterize the conditioning filter exactly. The main advantage of VAMPIRE over methods like SPIDER or FROG is that no relative-phase ambiguities appear. Complex-shaped pulses with zeros in the spectral intensity profile can be reconstructed with VAMPIRE. For the simultaneous measurement of two signals, the conditioning filter must be characterized beforehand. This can be done by the VAMPIRE technique itself because the two signals in figure 2 can simply be swapped for that purpose in the experiment. The complex transfer function of the conditioning filter can be calculated from the spectral phase changes of the signals. The new reconstruction algorithm has several advantages. The fact that all solutions of the one-dimensional phase problems in the first step in figure 4 are unique enables the fields to be retrieved without stagnation. The algorithm generally converges even for complex and noisy pulses. The performance is especially good for highly resolved VAMPIRE grids. Note that iterative techniques such as the Gerchberg–Saxton algorithm [18] can have difficulties in retrieving measured data due to stagnation. We solved the problem by modifying the function G and using the overdetermination of the considered system of equations. Moreover, we have introduced a new feature for the reconstruction. This is about increasing the resolution by the use of the CZT.

Acknowledgments

We are grateful for the financial support which we received from the Deutsche Forschungsgemeinschaft (DFG) through the DFG research group ‘Quantum Optics in Semiconductor Nanostructures’ (FOR 485). Further we thank the referees for their helpful comments.

References

- [1] Iaconis C and Walmsley I A 1998 Spectral phase interferometry for direct electric field reconstruction of ultrashort optical pulses *Opt. Lett.* **23** 792–4
- [2] Amat-Roldán I, Cormack I G, Loza-Alvarez P and Artigas D 2005 Measurement of electric field by interferometric spectral trace observation *Opt. Lett.* **30** 1063–5
- [3] Amat-Roldán I, Artigas D, Cormack I G and Loza-Alvarez P 2006 Simultaneous analytical characterisation of two ultrashort laser pulses using spectrally resolved interferometric correlations *Opt. Express* **14** 4538–51
- [4] Trebino R and Kane D J 1993 Using phase retrieval to measure the intensity and phase of ultrashort pulses: frequency-resolved optical gating *J. Opt. Soc. Am. A* **10** 1101–11
- [5] Trebino R 2002 *Frequency-Resolved Optical Gating: The Measurement of Ultrashort Laser Pulses* (Dordrecht, The Netherlands: Kluwer)
- [6] Wong V and Walmsley I A 1997 Ultrashort-pulse characterization from dynamic spectrograms by iterative phase retrieval *J. Opt. Soc. Am. B* **14** 944–9
- [7] Reid D T 1999 Algorithm for complete and rapid retrieval of ultrashort pulse amplitude and phase from sonogram *IEEE J. Quantum Electron.* **35** 1584–9
- [8] Keusters D, Tan H-S, O’Shea P, Zeek E, Trebino R and Warren W S 2003 Relative-phase ambiguities in measurements of ultrashort pulses with well-separated multiple frequency components *J. Opt. Soc. Am. B* **20** 2226–37
- [9] Iaconis C and Walmsley I A 1999 Self-referencing spectral interferometry for measuring ultrashort optical pulses *IEEE J. Quantum Electron.* **35** 501–9
- [10] Svanberg S 2001 Some applications of ultrashort laser pulses in biology and medicine *Meas. Sci. Technol.* **12** 1777–83
- [11] Hause A, Hartwig H, Seifert B, Stolz H, Böhm M and Mitschke F 2007 Phase structure of soliton molecules *Phys. Rev. A* **75** 063836
- [12] Seifert B, Nacke Ch, Kieseling F and Stolz H 2000 Femtosecond spectral interferometry of coherent secondary emission from quantum well excitons *Phys. Status Solidi (b)* **221** 413–7
- [13] Linden S, Giessen H and Kuhl J 1998 XFROG—a new method for amplitude and phase characterization of weak ultrashort pulses *Phys. Status Solidi B* **206** 119–224
- [14] Hirasawa M, Nakagawa N, Yamamoto K, Morita R, Shigekawa H and Yamashita M 2002 Sensitivity improvement of spectral phase interferometry for direct electric-field reconstruction for the characterization of low-intensity femtosecond pulses *Appl. Phys. B* **74** S225–9
- [15] Morita R, Hirasawa M, Karasawa N, Kusaka S, Nakagawa N, Yamane K, Li L, Suguro A and Yamashita M 2002 Sub-5 fs optical pulse characterization *Meas. Sci. Technol.* **13** 1710–20
- [16] Seifert B, Stolz H and Tasche M 2004 Nontrivial ambiguities for blind frequency-resolved optical gating and the problem of uniqueness *J. Opt. Soc. Am. B* **21** 1089–97
- [17] Kane D J 1998 Real-time measurement of ultrashort laser pulses using principal component generalized projections *IEEE J. Sel. Top. Quantum Electron.* **4** 278–84
- [18] Gerchberg R W and Saxton W O 1972 A practical algorithm for the determination of phase from image and diffraction plane pictures *Optik* **35** 237–46
- [19] Seifert B, Stolz H, Donatelli M, Langemann D and Tasche M 2006 Multilevel Gauss–Newton methods for phase retrieval problems *J. Phys. A: Math. Gen.* **39** 4191–206
- [20] Bluestein L I 1968 A linear filtering approach to the computation of the discrete Fourier transform *Northeast Electronics Research and Engineering Meeting Record* vol 10 pp 218–9
- [21] Rabiner L, Schafer R and Rader C 1969 The chirp z-transform algorithm *IEEE Trans. Audio Electroacoust.* **17** 86–92
- [22] Schott AG 2002 *Glass Catalog* (Mainz, Germany)
- [23] DeLong K W, Trebino R and White W E 1995 Simultaneous recovery of two ultrashort laser pulses from a single spectrogram *J. Opt. Soc. Am. B* **12** 2463–6